FEBS Letters 580 (2006) 399–409

Thr[199] phosphorylation targets nucleophosmin to nuclear speckles and represses pre-mRNA processing

Pheruza Tarapore[a], Kazuya Shinmura[a], Hitoshi Suzuki[b], Yukari Tokuyama[a], Song-Hee Kim[a], Akila Mayeda[b], Kenji Fukasawa[a,*]

[a] *Department of Cell Biology, University of Cincinnati College of Medicine, P.O. Box 670521, 3125 Eden Ave, Cincinnati, OH 45267-0521, USA*
[b] *Department of Biochemistry and Molecular Biology, University of Miami Miller School of Medicine, P.O. Box 016129, Miami, FL 33101-6129, USA*

Received 17 November 2005; revised 5 December 2005; accepted 7 December 2005

Available online 19 December 2005

Edited by Ivan Sadowski

Abstract **Nucleophosmin (NPM) is a multifunctional phosphoprotein, being involved in ribosome assembly, pre-ribosomal RNA processing, DNA duplication, nucleocytoplasmic protein trafficking, and centrosome duplication. NPM is phosphorylated by several kinases, including nuclear kinase II, casein kinase 2, Polo-like kinase 1 and cyclin-dependent kinases (CDK1 and 2), and these phosphorylations modulate the activity and function of NPM. We have previously identified Thr[199] as the major phosphorylation site of NPM mediated by CDK2/cyclin E (and A), and this phosphorylation is involved in the regulation of centrosome duplication. In this study, we further examined the effect of CDK2-mediated phosphorylation of NPM by using the antibody that specifically recognizes NPM phosphorylated on Thr[199]. We found that the phospho-Thr[199] NPM localized to dynamic sub-nuclear structures known as nuclear speckles, which are believed to be the sites of storage and/or assembly of pre-mRNA splicing factors. Phosphorylation on Thr[199] by CDK2/cyclin E (and A) targets NPM to nuclear speckles, and enhances the RNA-binding activity of NPM. Moreover, phospho-Thr[199] NPM, but not unphosphorylated NPM, effectively represses pre-mRNA splicing. These findings indicate the involvement of NPM in the regulation of pre-mRNA processing, and its activity is controlled by CDK2-mediated phosphorylation on Thr[199].**

Keywords: Nucleophosmin; mRNA splicing; CDK2; Cyclin E; Nuclear speckles; Splicing factor

1. Introduction

Nucleophosmin (NPM), also known as B23, NO38 or numatrin, is a multifunctional phosphoprotein, and has been implicated in a wide variety of cellular events, including ribosome assembly and pre-ribosomal RNA processing in nucleolus [1–4], DNA duplication [5–7], nucleocytoplasmic protein trafficking through directly binding to the nuclear localization signals (NLS) of the target proteins [8–11], and centrosome duplication [12,13]. In addition, NPM has been shown to possess interesting properties, including RNA-binding and molecular chaperoning activities [14–17]. NPM is phosphorylated by several different kinases, including casein kinase 2 (CK2), nuclear kinase II, Polo-like kinase 1 (PLK1) and cyclin-dependent kinases (CDK1/cyclin B, CDK2/cyclin E, and CDK2/cyclin A) [12,13,17–22]. Phosphorylation by CK2 increases NPM's affinity to the NLS sequences derived from the SV40 large T antigen and the HIV Rev protein [10,11] as well as to modulate its molecular chaperoning activity, especially for its interaction with target proteins [21]. Phosphorylation of NPM on Ser[4] by PLK1 has been shown to play a role in numeral homeostasis of centrosomes as well as cytokinesis [22]. Phosphorylation by CDK2/cyclin E (and A) on Thr[199] of NPM is critical for the regulation of centrosome duplication by affecting its binding affinity to centrosomes [13].

It has been shown that NPM binds and alters the secondary structure of RNA [15,17]. Moreover, the RNA-binding activity of NPM is controlled by phosphorylation. For instance, CDK1/cyclin B phosphorylates NPM on several residues, which results in a decrease in the RNA-binding affinity of NPM [17]. These observations suggest the role of NPM in RNA transcription, metabolism, and/or processing. Indeed, NPM was co-purified from HeLa cell nuclear extracts with general splicing activator RNPS1, which physically interacts with serine/arginine-rich (SR) splicing factors, pinin, human Tra2β, and CK2 to regulate splicing in vivo [23–25], suggesting its potential association with pre-mRNA splicing. Pre-mRNA splicing occurs in a macromolecular complex known as the spliceosome, which consists of five small nuclear ribonuclear particles (snRNPs) and a large number of non-snRNP protein splicing factors (reviewed in [26,27]). The phosphorylation state of splicing factors appears to be critical for at least two events during the pre-mRNA splicing process; (1) spliceosome formation and (2) selection of pre-mRNA splice sites (reviewed in [28]). Pre-mRNA splicing factors are mostly confined to 20–50 irregularly shaped nuclear speckles within the nucleoplasm, which are believed to be the sites of storage and/or assembly of pre-mRNA splicing factors (reviewed in [29]). Ultrastructural studies have revealed that the nuclear speckles consist of interchromatin granule clusters (IGCs) and perichromatin fibrils (PFs) (reviewed in [30,31]). IGCs are composed of particles measuring 20–25 nm in diameter, and they contain numerous factors that are involved in mRNA synthesis and processing. IGC constituents include small nuclear ribonucleoprotein particles (snRNPs), SR splicing factors, and hyperphosphorylated form of the large subunit of RNA polymerase II [32]. Despite the presence of splicing factors in IGCs, pre-mRNA processing does not occur within these structures, but rather at PFs, which are found at the periphery of or at some distance away from IGCs [33].

*Corresponding author. Fax: +1 513 558 4454.
E-mail address: kenji.fukasawa@uc.edu (K. Fukasawa).

0014-5793/$32.00
doi:10.1016/j.febslet.2005.12.022

In this communication, we exploited the biological significance of the Thr[199] phosphorylation of NPM in cellular event(s) other than centrosome duplication by the use of the antibody that specifically recognizes NPM phosphorylated on Thr[199] (phospho-Thr[199] NPM). We found that phospho-Thr[199] NPM localizes at nuclear speckles. As expected from the cell cycle phase-specific activation of CDK2/cyclin E as well as CDK2/cyclin A, appearance of phospho-Thr[199] NPM occurs in a cell cycle-dependent manner. Moreover, CDK2/cyclin E-mediated phosphorylation of NPM significantly enhances its RNA-binding affinity, and represses pre-mRNA splicing in vitro. These findings suggest the involvement of NPM in the regulation of pre-mRNA processing, which is modulated by CDK2/cyclin E (and A)-mediated phosphorylation on Thr[199].

2. Materials and methods

2.1. Cell and transfection

Wild-type mouse skin fibroblasts (MSFs) were prepared from abdominal skins of an 8-week-old C57L male mouse, and maintained in complete medium [DMEM supplemented with 10% fetal bovine serum (FBS), penicillin (100 U/ml) and streptomycin (100 μg/ml)] in an atmosphere containing 10% CO_2. Plasmid transfection was performed using Fugene 6 reagent (Roche).

2.2. Antibodies

Anti-pan NPM mouse monoclonal antibody is a gift from Dr. P.K. Chan (Baylor College of Medicine). Anti-phospho-Thr[199] rabbit polyclonal antibody (Cell Signaling Technology) was generated against a synthetic phospho-peptide around Thr[199] of human NPM. The antibodies were purified by protein A and affinity chromatography. Anti-cyclin E (M-20), anti-cyclin A (C-19), anti-cyclin B (SC-55), anti-hnRNP I and anti-SF2/ASF antibodies were purchased from Santa Cruz Biotechnology. Anti-FLAG (M2) and anti-α-tubulin (DM1A) antibodies were purchased from Sigma Immunochemicals. Anti-T7-tag antibody was purchased from Novagen. Generation of mouse anti-SC35 antibody was previously described [34].

2.3. Immunoblot analysis

Cells were washed three times with PBS and lysed in SDS/NP-40 lysis buffer [1% SDS, 1% NP-40, 50 mM Tris (pH 8.0), 150 mM NaCl, 4 mM Pefabloc SC (Roche), 2 μg/ml leupeptin, 2 μg/ml aprotinin]. The lysates were boiled for 5 min, and cleared by a 10 min centrifugation at 20 000 × *g* at 4 °C. The supernatant was denatured at 95 °C for 5 min in sample buffer [2% SDS, 10% glycerol, 60 mM Tris (pH 6.8), 5% β-mercaptoethanol, 0.01% bromophenol blue]. Samples were resolved by SDS–PAGE, and transferred onto Immobilon-P sheets (Millipore). The blots were incubated in blocking buffer [5% (wt/vol) nonfat dry milk in Tris-buffered saline (TBS) + Tween 20 (TBS-T)] for 1 h at room temperature. The blots were incubated with primary antibody for overnight at 4 °C, followed by incubation with horseradish peroxidase-conjugated secondary antibody for 1 h at room temperature. The antibody-antigen complex was visualized by ECL chemiluminescence (Amersham Biosciences).

2.4. Indirect immunofluorescence

Cells grown on coverslips were fixed with 10% formalin/10% methanol for 20 min at room temperature. The cells were permeabilized with 1% NP-40 in PBS for 5 min, followed by incubation with blocking solution [10% normal goat serum in PBS] for 1 h. Cells were then probed with primary antibodies for 1 h, and antibody-antigen complexes were detected with either Alexa Fluor 488- or Alexa Fluor 594-conjugated goat secondary antibody (Molecular Probes) by incubation for 1 h at room temperature. The coverslips were washed three times with PBS after each incubation, and then counterstained with 4′,6-diamidino-2-phenylindole (DAPI). Immunostained cells were examined under a fluorescence microscope (Zeiss Axioplan 2 Imaging, 60× objective lens) or confocal microscope (Zeiss LSM510, 63× objective lens).

2.5. In vitro kinase assay

GST, GST-NPM/wt, or GST-NPM/T199A were incubated with baculovirally purified active CDK2/cyclin E [35] or CK2 (New England Biolabs). The enzymatic activities of both CDK2/cyclin E and CK2 were confirmed by in vitro kinase reactions in the presence of [γ-^{32}P]ATP using GST-NPM/wt as a substrate. The in vitro kinase reactions were performed in 10 mM PIPES buffer in the presence of ATP at 32 °C for 30 min. The reaction samples were resolved by SDS–PAGE.

2.6. Alkaline phosphatase treatment

Cells grown on coverslips were fixed with 100% methanol for 10 min at −20 °C. Cells were then air-dried, and re-hydrated in PBS for 10 min at room temperature. Cells were incubated in the solution [100 mM glycine (pH 10.4)] containing 10 units of alkaline phosphatase type IV (Sigma) for 2 h at 37 °C. The control cells were incubated in the solution without alkaline phosphatase.

2.7. RNA binding assay

The assay was performed as previously described [17]. Briefly, RNA was extracted from MSFs using TRIZOL (Gibco BRL). GST-NPM proteins were subjected to an in vitro kinase assay with CDK2/cyclin E, and mixed with RNA for 30 min at room temperature. The samples were loaded onto 15–40% sucrose gradient [20 mM Tris (pH 7.4), 50 mM NaCl, 0.5 mM PMSF, and 1 mM dithiothreitol], centrifuged at 39 000 rpm for 4 h, and fractions were collected from the bottom. The fractions were resolved in 10% SDS–PAGE for immunoblot analysis, and on 1% agarose-formaldehyde gel electrophoresis for Northern blot analysis using ^{32}P-labeled 18S rRNA DNA probe (Ambion).

2.8. Northwestern analysis

Bacterially purified GST, GST-NPM/wt, GST-NPM/T199A, or GST-NPM/T199D proteins were phosphorylated with CDK2/cyclin E, and re-purified. The proteins were separated by SDS–PAGE and transferred to a membrane. The membrane was blocked with 5% non-fat dry milk in RNA-binding buffer (RBB) [20 mM Tris–HCl (pH 7.5), 60 mM KCl, 1 mM $MgCl_2$, 0.2 mM EDTA, 10% glycerol] containing 2 μg/ml yeast tRNA for 1 h, and then incubated in the RBB containing 0.25% non-fat dry milk, 2 μg/ml yeast tRNA, 1 U/ml RNase inhibitor, and ^{32}P-labeled β-globin pre-mRNA for 16 h. The membrane was washed, air-dried, and autoradiographed.

2.9. In vitro splicing assay

The m^{7}GpppG-capped ^{32}P-labeled pre-mRNA was made by run-off transcription of linearized β-globin template DNA with SP6 RNA polymerase, which was used as a substrate for in vitro splicing assay in HeLa cell nuclear extract [36]. Bacterially purified GST, GST-NPM/wt, GST-NPM/T199A, or GST-NPM/T199D proteins were phosphorylated with CDK2/cyclin E, and re-purified. The mock or CDK2/cyclin E phosphorylated GST, GST-NPM/wt, GST-NPM/T199A, or GST-NPM/T199D was added to splicing reactions (in 25 μl) with 20 fmol of ^{32}P-labeled β-globin pre-mRNA and incubated at 30 °C for 2–3 h. The spliced products were analyzed by denaturing 5.5% PAGE and autoradiography.

3. Results

3.1. NPM phosphorylated on Thr[199] localizes in a speckled pattern in the nuclei

NPM is phosphorylated on Thr[199] primarily by CDK2/cyclin E and A, and this phosphorylation is important in the regulation of centrosome duplication [13]. Since centrosome duplication occurs in coordination with other cell cycle events, and NPM is involved in a variety of cellular events, it is possible that CDK2-mediated phosphorylation of NPM may affect more than one cellular event. To test this possibility, we obtained an antibody, which was generated against phospho-Thr[199] of NPM. We first tested the specificity of the anti-phospho-Thr[199] NPM antibody. The bacterially purified wild-type

NPM proteins fused to GST (GST-NPM/wt) were subjected to an in vitro kinase assay with CDK2/cyclin E. Since CK2 has been shown to be another major kinase that phosphorylates NPM on the residues other than Thr[199] [21], in vitro kinase reaction was also performed with CK2 as a control. We also included a NPM mutant whose Thr[199] residue was replaced with Ala (GST-NPM/T199A) as well as GST alone as controls. The reaction samples were immunoblotted using phospho-Thr[199] NPM antibody (Fig. 1A, panel a). The same blot was stained with Coomassie blue (panel b), showing that all reaction samples contain similar levels of either GST-NPM/wt or GST-NPM/T199A. GST-NPM/wt phosphorylated by CDK2/cyclin E was readily detected by the anti-phospho-Thr[199] NPM antibody (lane 8). It should be noted that the GST-NPM/wt phosphorylated by CDK2/cyclin E showed a slightly faster migration than the unphosphorylated form (lane 17), which is consistent with the previous observation [12]. In contrast to wild-type GST-NPM, neither GST (lane 7) nor GST-NPM/T199A (lane 9) was recognized by the anti-phospho-Thr[199] NPM antibody. Phosphorylation of GST-NPM/

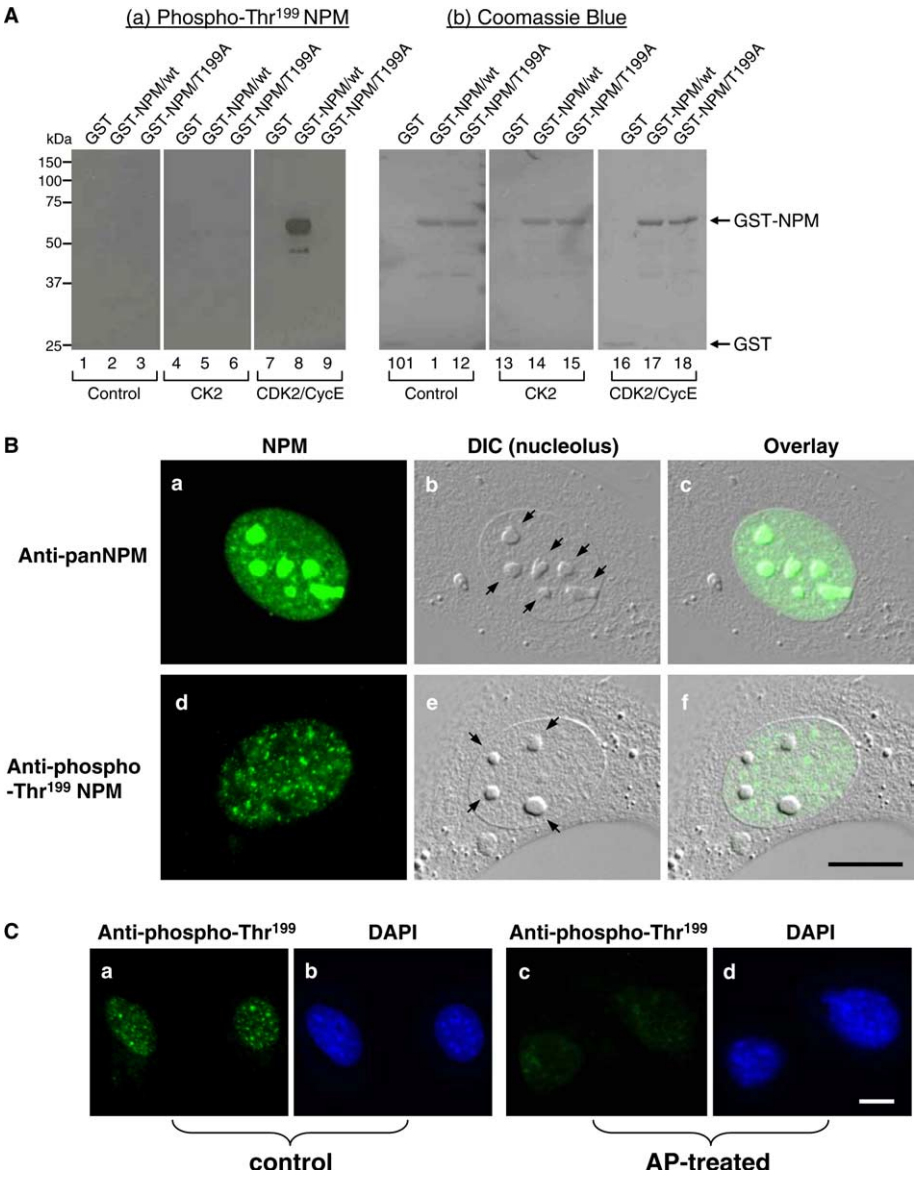

Fig. 1. Phospho-Thr[199] NPM is distributed in a speckled pattern within the nucleus. (A) Characterization of anti-phospho-Thr[199] NPM antibody. Wild-type and Ala-substitution mutant NPM fused to GST (GST-NPM/wt and GST-NPM/T199A, respectively) as well as GST alone was subjected to an in vitro kinase assay with either CK2 or CDK2/cyclin E. The reactions were resolved in SDS–PAGE and immunoblotted using anti-phospho-Thr[199] NPM antibody (left panel). Coomassie blue staining of the same gel is shown in the right. Only the wild-type NPM phosphorylated by CDK2/cyclin E was detected by anti-phospho-Thr[199] NPM antibody (lane 8), demonstrating the specificity of this antibody. (B) MSFs were fixed and immunostained with either anti-panNPM monoclonal (panels a–c) or anti-phospho-Thr[199] NPM polyclonal (panels d–f) antibodies. The nucleoli are depicted by differential interference contrast microscopy (indicated by arrows, panels b and e). Panels c and f show the overlay images. Scale bar: 10 μm. (C) After fixation, cells were treated with alkaline phosphatase (AP) (see Section 2). The control cells were incubated in the solution without alkaline phosphatase. The AP-treated (panels c and d) and mock-treated MSFs (panels a and b) were then immunostained with anti-phospho-Thr[199] NPM antibody (panels a and c). Cells were also stained for DNA with DAPI (panels b and d). In the AP-treated cells, anti-phospho-Thr[199] NPM antibody no longer detected the speckled pattern of signals (panel c). Scale bar: 10 μm.

wt (lane 5) and GST-NPM/T199A (lane 6) by CK2 was not detected by this antibody. Thus, the anti-phospho-Thr^{199} NPM antibody is specific to NPM phosphorylated on Thr^{199} by CDK2.

We next examined whether phospho-Thr^{199} NPM shows any specific subcellular localization by immunostaining primary skin fibroblasts (MSFs) derived from adult mice with the anti-phospho-Thr^{199} NPM antibody. We also immunostained MSFs with anti-panNPM monoclonal antibody raised against a purified NPM protein, which reacts with both phosphorylated and non-phosphorylated forms of NPM [12]. The anti-panNPM antibody detected NPM primarily in the nucleolus and to lesser extent in the nucleoplasm as scattered small dot-like structures (Fig. 1B, panels a–c). In contrast, anti-phospho-Thr^{199} NPM antibody did not detect NPM in the nucleolus, but detected NPM in distinct intranuclear structures (speckles) as well as in diffuse regions throughout the nucleoplasm (Fig. 1B, panels d–f). The speckles detected by the anti-phospho-Thr^{199} NPM antibody are clearly distinct from nucleoli that are visualized in the differential interference contrast (DIC) image of the cell (Fig. 1B, panel e, nucleoli are indicated by arrows).

To further confirm the specificity of the immunostaining pattern of the anti-phospho-Thr^{199} NPM antibody, we treated the fixed MSFs with alkaline phosphatase and immunostained with the anti-phospho-Thr^{199} NPM antibody. The control untreated MSFs (Fig. 1C, panel a) showed the speckled as well as the diffuse staining pattern similar to the cell shown in Fig. 1B (panel d). However, the anti-phospho-Thr^{199} NPM antibody failed to detect antigens in the alkaline phosphatase-treated cells, demonstrating that this antibody is indeed detecting the phosphorylated epitope (Fig. 1C, panel c).

3.2. Kinetic analysis of phospho-Thr^{199} NPM during the cell cycle

Since CDK2/cyclin E is activated during late G1 phase of the cell cycle, we tested the changes in the levels of phospho-Thr^{199} NPM during the cell cycle. We first synchronized MSFs by serum starvation, followed by serum stimulation. At every 5 h after serum-stimulation for a period of 20 h, cells were fixed and examined by anti-phospho-Thr^{199} NPM immunostaining (Fig. 2A). To monitor the cell cycle progression, cells were cultured in parallel in the presence of BrdU (Fig. 2C). Under a serum-starved condition, there was little or no phospho-Thr^{199} NPM staining as expected. Between 5 and 10 h after serum stimulation, weak yet detectable signals of phospho-Thr^{199} NPM staining were observed in some cells. At 20 h, strong signals of phospho-Thr^{199} NPM staining were detected in the majority of cells. To quantitate the cell cycle-dependent emergence of phospho-Thr^{199} NPM, the images taken by laser scanning confocal microscopy were subjected to the computational morphometric measurements (Fig. 2B). The intensity of the phospho-Thr^{199} NPM signals gradually increased during serum stimulation, and importantly the rate of the increase was closely parallel to the rate of BrdU incorporation (Fig. 2C). Considering that CDK2/cyclin E is activated prior to S phase entry, these results indicate that appearance of phospho-Thr^{199} NPM in the nuclear speckle pattern is mediated by activated CDK2/cyclin E.

To corroborate the above observations, we examined the phospho-Thr^{199} NPM protein level in MSFs after serum stimulation by immunoblot analysis (Fig. 2D, top panel). At 0 h, no phospho-Thr^{199} NPM was detected. As the cell cycle progressed (5, 10, 15 h), we detected low levels of phospho-Thr^{199} NPM. At 20 h of serum stimulation, the level of phospho-Thr^{199} NPM increased dramatically. These results are consistent with the changes in the level of phospho-Thr^{199} NPM during G1 progression observed immunocytochemically. The changes in the level of phospho-Thr^{199} NPM was not due to the changes in the overall NPM protein level, since immunoblot analysis using anti-panNPM antibody showed no significant change in the total NPM protein level during 20 h of serum stimulation (Fig. 2D, bottom panel).

The level of phospho-Thr^{199} NPM did not saturate and continued to increase at 20 h of serum stimulation, while ~80% of the cells had entered S-phase (Fig. 2B and C). Because CDK2/cyclin E activation peaks at G1/S transition, the failure to saturate NPM phosphorylation on Thr^{199} raises the possibility that kinase(s) other than CDK2/cyclin E may also catalyze the phosphorylation of NPM on Thr^{199}. Since CDK2/cyclin A can phosphorylate NPM on Thr^{199} [13] and CDK2/cyclin A activation occurs during S-phase [37], it is possible that CDK2/cyclin A may be responsible for continuous phosphorylation of NPM on Thr^{199}. To test this, the lysates prepared from cells at every 5 h for a total of 20 h during serum-stimulation were subjected to immunoblot analysis using anti-cyclin E, anti-cyclin A, and anti-cyclin B antibodies (Fig. 2E). The level of cyclin E peaked at 15 h (top panel), while the increase in the level of cyclin A was detected between 15 and 20 h (second panel), indicating that CDK2/cyclin E initiates phosphorylation of NPM on Thr^{199}, and CDK2/cyclin A may take over Thr^{199} phosphorylation of NPM in late G1 and S. Cyclin B was not detectable at 20 h (third panel), indicating that CDK1/cyclin B is not responsible for generation of the anti-phospho-Thr^{199} NPM antibody epitope at 20 h during serum-stimulation. Indeed, it has been shown that CDK1/cyclin B phosphorylates NPM on the residues other than Thr^{199} [13].

3.3. Phospho-Thr^{199} NPM localizes to nuclear speckles

The unique sub-nuclear localization of phospho-Thr^{199} NPM prompted us to search for other nuclear proteins with similar localization patterns. The pre-mRNA splicing machinery, which primarily consists of small nuclear ribonucleoprotein particles (snRNPs) and many non-snRNP protein factors, is known to sub-nuclearly localize in a speckle pattern known as "nuclear speckles" [29]. A member of SR protein family SC35, a non-snRNP spliceosome component that is essential for spliceosome assembly and function, has been used as a marker protein for identifying nuclear speckles [38,39]. We noticed that the immunostaining pattern of SC35 shown in previous studies resembles that of phospho-Thr^{199} NPM. In addition, biochemical co-purification of NPM along with splicing activator RNPS1 from HeLa cell nuclear extracts [25] raises the possibility that phospho-Thr^{199} NPM may localize to nuclear speckles. To test this possibility, we co-immunostained MSFs with anti-phospho-Thr^{199} NPM and anti-SC35 antibodies (Fig. 3A). We found that phospho-Thr^{199} NPM co-localized to many of the speckles identified by anti-SC35 antibody. Similarly, we found co-localization of the transiently transfected T7-tagged RNPS1 and phospho-Thr^{199} NPM in a speckled pattern (Fig. 3B). These results demonstrate that NPM localizes to nuclear speckles, and co-localization of

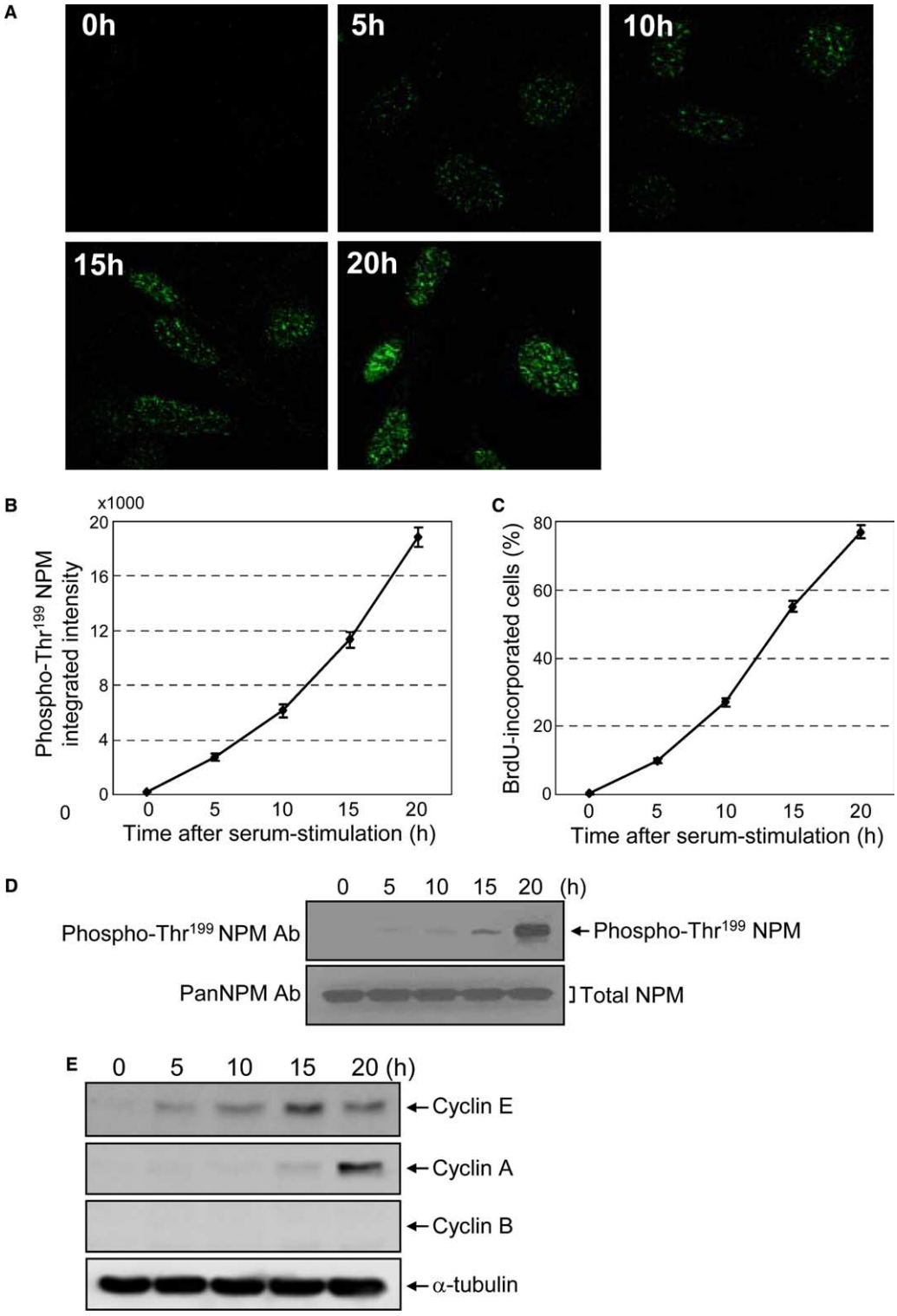

Fig. 2. Cell-cycle dependent changes in the level of phospho-Thr[199] NPM. (A) MSFs were serum starved for 48 h, followed by serum stimulation with medium containing 20% FBS. At indicated time points, cells were immunostained using anti-phospho-Thr[199] NPM antibody. (B) The immunostained images taken by confocal microscopy in A were quantitated for phospho-Thr[199] NPM signals by integrated morphometry analysis using Metamorph software program (Universal Imaging Corp.). (C) In parallel, MSFs were examined for BrdU incorporation using the BrdU-labeling kit (Roche). After serum starvation for 48 h, MSFs were serum stimulated with medium containing 20% FBS in the presence of BrdU. MSFs were then immunostained with anti-BrdU antibody. The rate of BrdU incorporation was determined by examining >300 cells. (D) MSFs were serum starved for 48 h, followed by serum stimulation. The whole cell lysates were prepared at indicated time points and immunoblotted with anti-phospho-Thr[199] NPM antibody (top panel) as well as anti-panNPM antibody (bottom panel). It should be noted that the running condition of the SDS–PAGE in this analysis does not allow the band separation of phosphorylated and unphosphorylated NPM by anti-panNPM antibody. (E) The lysates described above in (D) were immunoblotted with anti-cyclin E (top panel), anti-cyclin A (second panel) and anti-cyclin B (third panel) antibodies. As a loading control, the lysates were immunoblotted with anti-α-tubulin antibody.

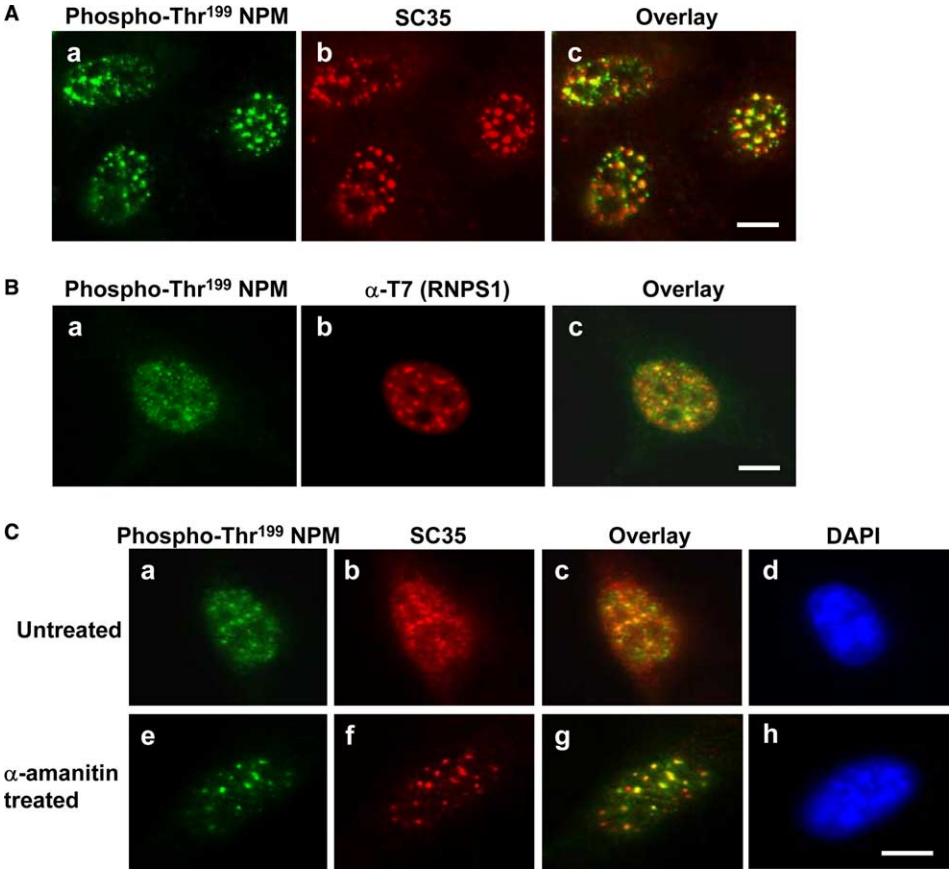

Fig. 3. Phospho-Thr^{199} NPM localizes at nuclear speckles. (A) Phospho-Thr^{199} NPM co-localizes with SC35 at nuclear speckles. MSFs under an optimal growth condition were co-immunostained with rabbit anti-phospho-Thr^{199} NPM (panel a) and mouse anti-SC35 (panel b) antibodies. Antigen-antibody complexes were detected with Alexa Fluor 488 goat anti-rabbit IgG (green) and Alexa Fluor 594 goat anti-mouse IgG (red) antibodies. Panel c is the overlay image, showing a high degree of co-localization of phospho-Thr^{199} NPM and SC35. Scale bar: 10 μm. (B) Phospho-Thr^{199} NPM co-localizes with RNPS1 at nuclear speckles. MSFs were transiently co-transfected with a plasmid encoding T7 epitope-tagged RNPS1 and a plasmid encoding a puromycin resistance gene (pBabe/puro) at a molar ratio of 20:1. The puromycin-resistant cells were pooled and replated on coverslips and further cultured in fresh complete medium for 24 h. Cells were then co-immunostained with rabbit anti-phospho-Thr^{199} NPM (panel a) and mouse anti-T7 tag (panel b) antibodies. Antigen-antibody complexes were detected as described in (A). The co-localization of phospho-Thr^{199} NPM and RNPS1 was detected as yellow color in the overlay image (panel c). Scale bar: 10 μm. (C) Co-migration of phospho-Thr^{199} NPM and SC35 to enlarged speckles upon inhibition of transcription. MSFs were treated with α-amanitin (50 μg/ml) for 5 h. The control MSFs were untreated. Cells were then fixed and immunostained with anti-phospho-Thr^{199} NPM and anti-SC35 antibodies as described above. The nuclei were also counterstained with DAPI (panels d and h). Panels c and g are the overlay images. In control cells, phospho-Thr^{199} NPM (panel a) and SC35 (panel b) distributed in a speckled pattern along with a diffuse staining. In contrast, in α-amanitin treated cells, both phospho-Thr^{199} NPM and SC35 redistributed to enlarged and rounded speckles. Scale bar: 10 μm.

NPM with these representative splicing factors indicates the potential role of NPM in pre-mRNA processing.

Nuclear speckles are structurally dynamic, changing the constituent proteins depending on the transcription activity of the cell. Upon transcription activation, pre-mRNA splicing factors such as SC35 are recruited from interchromatin granule clusters (IGC) to perichromatin fibrils (PF) [40–42]. Thus, inhibition of transcription leads to a sub-nuclear redistribution of proteins involved in pre-mRNA processing and splicing factors including SC35. For instance, administration of RNA polymerase II inhibitor α-amanitin, which is commonly used for inhibition of transcription, results in appearance of enlarged rounded speckles of splicing factors and disappearance of diffuse connections between the speckles in the nucleoplasm [43,44]. To obtain further evidence for the nuclear speckle localization of phospho-Thr^{199} NPM, we tested whether phospho-Thr^{199} NPM would redistribute to enlarged speckles upon transcription inhibition along with SC35. To this end, MSFs were treated with α-amanitin, and co-immunostained with anti-phospho-Thr^{199} NPM and anti-SC35 antibodies. In the control untreated cells, we observed the co-localized speckle patterns of SC35 and phospho-Thr^{199} NPM along with diffuse staining (Fig. 3C, panels a–d). In the α-amanitin treated cells, as described previously [44], SC35 redistributed to enlarged rounded speckles and diffuse staining was no longer detected (panel f). We found that the phospho-Thr^{199} NPM redistributed together with SC35 to enlarged rounded speckles without any diffuse staining (panels e and g), demonstrating that NPM phosphorylated on Thr^{199} re-localizes along with other pre-mRNA processing factors, further indicating the potential involvement of NPM in pre-mRNA processing.

3.4. Thr^{199} phosphorylation targets NPM to nuclear speckles

As shown in Fig. 2A, phospho-Thr^{199} NPM is not found in the speckles in the serum-starved cells, but gradually accumulates during G1 and S progression. This observation raises the

question of whether CDK2-mediated phosphorylation of NPM occurs at nuclear speckles or CDK2-mediated phosphorylation targets NPM to nuclear speckles. To address this question, we transiently transfected FLAG-tagged non-phosphorylatable mutant NPM (NPM/T199A) and phospho-mimetic mutant NPM (NPM/T199D) into MSFs. As a control, a FLAG vector was transfected. The transfectants were immunostained with anti-FLAG and anti-SC35 antibodies (Fig. 4). No specific immunostaining by anti-FLAG antibody was observed in the vector-transfected cells (panels a–d). We found that the FLAG-T199A mutant failed to localize to the nuclear speckles detected by anti-SC35 antibody, but rather uniformly distributed within the nucleus with slightly more accumulation in nucleolus (panels e–h). In contrast, FLAG-T199D was more concentrated at typical nuclear speckles detected by anti-SC35 antibody (panels i–l). These results strongly indicate that Thr^{199} phosphorylation targets NPM to the speckle, and thus NPM translocates to the nuclear speckles upon Thr^{199} phosphorylation by CDK2/cyclin E (and A) during G1 progression and S-phase.

3.5. CDK2/cyclin E-mediated phosphorylation enhances the RNA-binding activity of NPM

Among the non-snRNP spliceosomal proteins, the members of the SR protein family (10 authentic human SR proteins have been identified to date) have been well characterized [45,46]. It has been shown that the RNA-binding activities of some SR proteins are modulated by phosphorylation [47–50]. Since NPM also possesses a RNA-binding activity [15–17], we examined whether Thr^{199} phosphorylation affects the RNA-binding activity of NPM. GST-NPM/wt and GST-NPM/T199A were subjected to an in vitro kinase assay with CDK2/cyclin E, and then incubated with total RNA extracted from MSFs. The reaction samples were subjected to a standard sucrose gradient sedimentation assay used for determination of general RNA binding of the protein. GST-NPM/wt alone and GST-NPM/wt subjected to a mock kinase reaction, were included as controls. The resulting fractions were collected and the total RNA elution profiles were determined. The RNA elution pattern of the control reaction (without GST-NPM and CDK2/cyclin E) is shown in the top panel of Fig. 5A. The RNA elution patterns of all the reaction samples were virtually identical to that of the control reaction. The same fractions were examined for NPM by immunoblot analysis. There was no significant difference in the elution patterns of NPM among GST-NPM/wt alone, non-phosphorylated GST-NPM/wt incubated with RNA, and GST-NPM/T199A after in vitro kinase reaction with CDK2/cyclin E (Fig. 5A, top three panels, fractions 2–8). In contrast, the phosphorylated GST-NPM/wt was eluted in fractions 2–10, demonstrating that CDK2-mediated

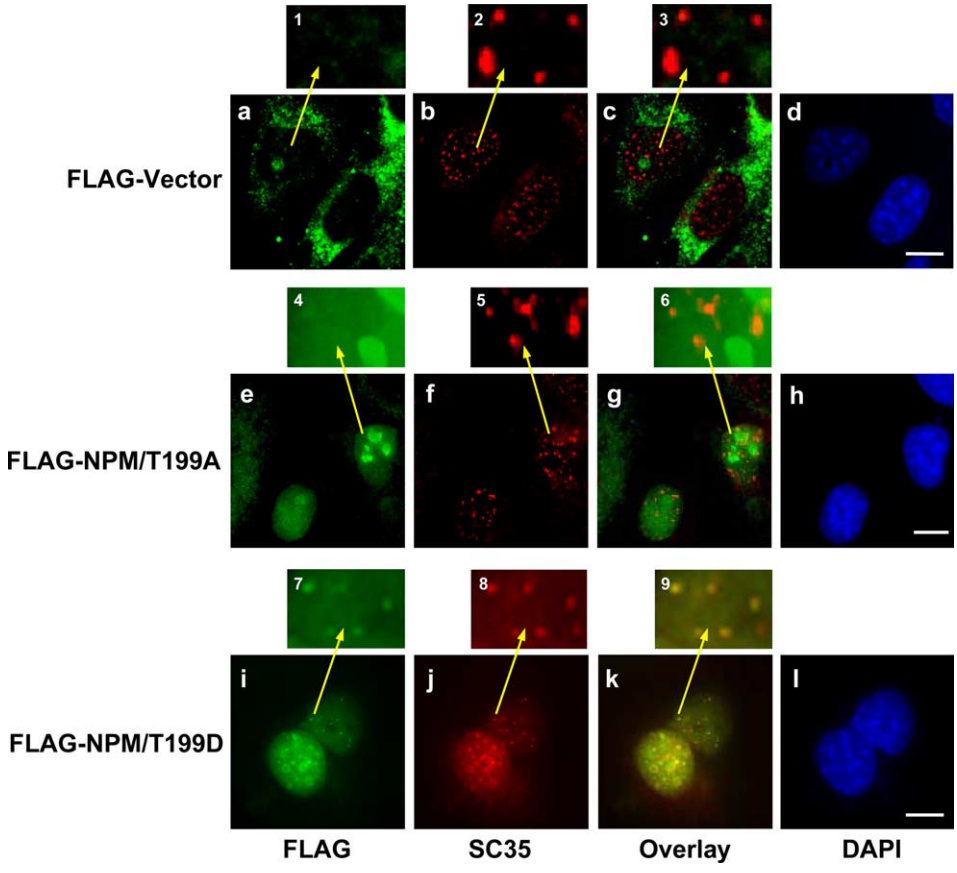

Fig. 4. Thr^{199} phosphorylation targets NPM to nuclear speckles. (A) MSFs were transiently transfected with either FLAG-tagged non-phosphorylatable mutant NPM (NPM/T199A) or phospho-mimetic mutant NPM (NPM/T199D). The FLAG vector was transfected as a control. The transfectants were co-immunostained with rabbit anti-FLAG and mouse anti-SC35 antibodies. Antigen-antibody complexes were detected with Alexa Fluor 488 goat anti-rabbit IgG (green) and Alexa Fluor 594 goat anti-mouse IgG (red) antibodies. Cells were also counterstained for DNA with DAPI. Panels 1–9 show the magnified images of the area indicated by arrows. Scale bar: 10 μm.

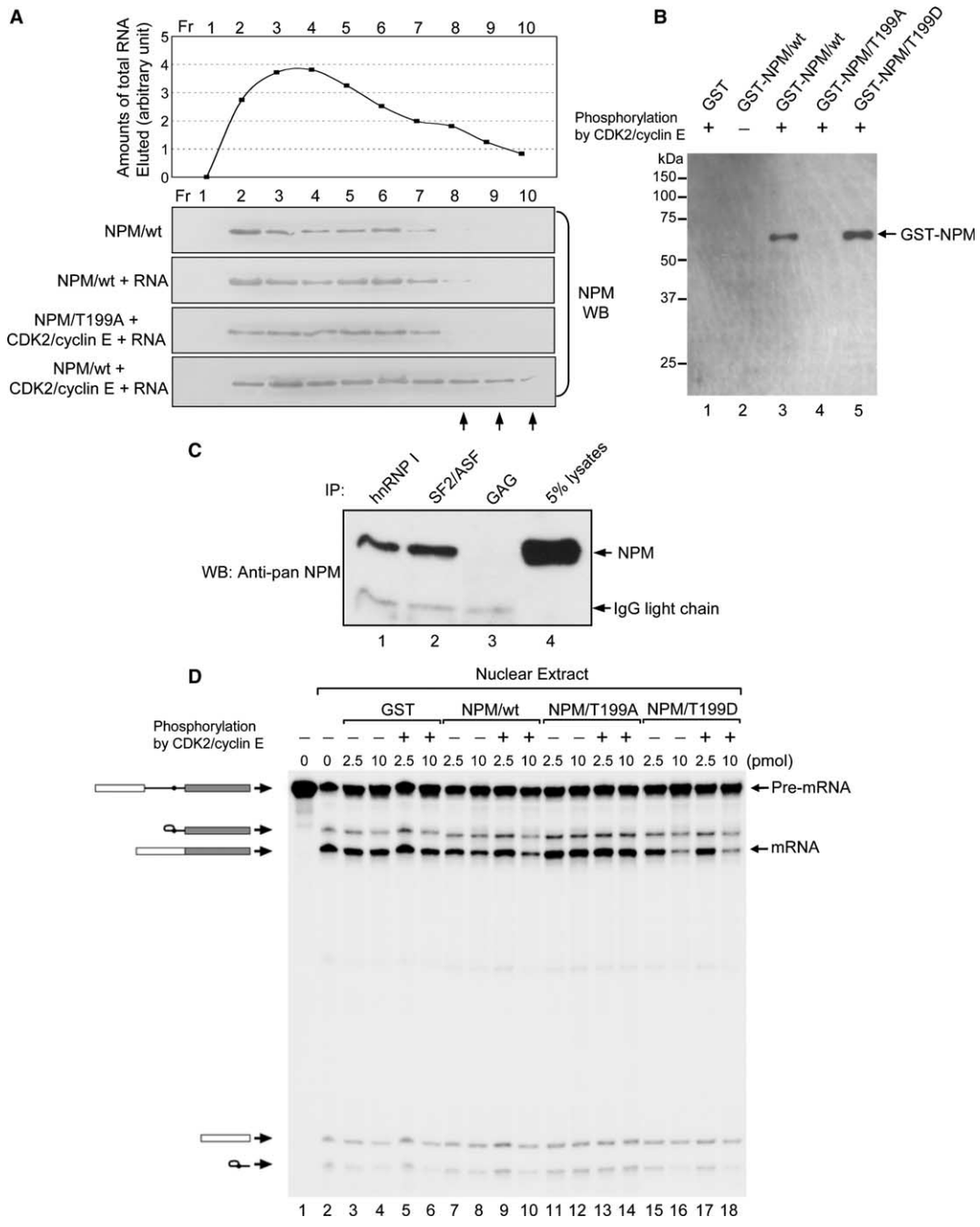

Fig. 5. Thr[199] phosphorylation enhances the RNA-binding activity of NPM, and phospho-Thr[199] NPM represses in vitro pre-mRNA splicing. (A) CDK2-mediated phosphorylation on Thr[199] enhances the RNA-binding activity of NPM. GST-NPM/wt and GST-NPM/T199A were subjected to an in vitro kinase assay with CDK2/cyclin E and incubated in the absence or presence of total RNA prepared from MSFs. The reaction samples were subjected to a 15–40% sucrose gradient fractionation, and the fractions were collected from the bottom of the tube. RNA as well as RNA/protein complexes were precipitated from each fraction. RNA from each fraction was resolved by 1% agarose-formaldehyde gel and probed for 18S rRNA (Ambion). It should be noted that probing for18S rRNA is a standard protocol with this experimental procedure to determine the elution profile of total RNA. The intensity of each band from the Northern blot was quantified using Metamorph software. The graph shown in the top is of the elution pattern of the total RNA without addition of neither NPM nor CDK2/cyclin E. The RNA elution patterns of all the reaction samples were virtually identical to that without reaction shown in the graph. Each fraction was then subjected to immunoblot analysis using anti-panNPM antibody (bottom four panels). The arrows point to the fractions showing apparent differences in the RNA-binding activity of NPM upon CDK2/cyclin E-mediated phosphorylation. (B) GST-NPM/wt proteins that were subjected to kinase reactions in the presence or absence of CDK2/cyclin E, as well as GST, GST-NPM/T199A and GST-NPM/T199D subjected to kinase reactions in the presence of CDK2/cyclin E were resolved in SDS–PAGE, and transferred to membrane. The membrane was then blotted with ^{32}P-labeled β-globin pre-mRNA, and autoradiographed. (C) NPM physically interacts with splicing factors. The HeLa nuclear extracts were immunoprecipitated with anti-hnRNP I and anti-SF2/ASF antibodies. As a control, the extracts were immunoprecipitated with anti-viral gag protein antibody. The immunoprecipitates were immunoblotted with anti-panNPM antibody. As a reference, 5% of the extracts used for immunoprecipitation were included in the immunoblot analysis. (D) Phospho-Thr[199] NPM represses in vitro pre-mRNA splicing. ^{32}P-labeled β-globin pre-mRNA was incubated with HeLa nuclear extract and indicated amounts of GST, GST-NPM/wt, GST-NPM/T199A or GST-NPM/T199D subjected to kinase reactions either in the presence or absence of CDK2/cyclin E. The spliced products were analyzed by 5.5% polyacrylamide/7 M urea gel, and autoradiographed. As controls, ^{32}P-labeled β-globin pre-mRNA samples without splicing reaction (lane 1) and with splicing reaction without addition of GST or GST-fusion proteins (lane 2) were included. The experiment was repeated three times, and obtained similar results in all the experiments.

phosphorylation of NPM substantially increased its RNA-binding affinity (bottom panel). It should be noted here that the elution of NPM in the wide fraction range probably reflects the property of NPM to oligomerize [51,52]. However, CDK2-mediated phosphorylation does not appear to affect the ability of NPM to oligomerize (P. Tarapore, unpublished observation), and thus the changes in the elution pattern of in vitro phosphorylated NPM is not due to the changes in its oligomerization property.

To corroborate the above finding, we performed Northwestern blot analysis of GST-NPM/wt with or without kinase reaction with CDK2/cyclin E as well as GST-NPM/T199A and GST-NPM/T199D mutants using the ^{32}P-labeled β-globin pre-mRNA as a probe (Fig. 5B). The unphosphorylated GST-NPM/wt failed to bind to the probe (lane 2), while GST-NPM/wt phosphorylated by CDK2/cyclin E were readily detected by the probe (lane 3). Similarly, GST-NPM/T199A non-phosphorylatable mutant failed to bind to the probe (lane 4), while GST-NPM/T199D phospho-mimetic mutant efficiently bound to the probe (lane 5). These results further indicate that the RNA-binding activity of NPM is greatly enhanced by CDK2-mediated phosphorylation on Thr^{199}.

3.6. Repression of pre-mRNA splicing by NPM phosphorylated on Thr^{199}

It has been shown that phosphorylation/dephosphorylation plays a critical role in the regulation of the activities of proteins involved in pre-mRNA splicing [47–50]. We have shown that (i) NPM localizes to nuclear speckles likely as a part of spliceosome complexes, (ii) Thr^{199} phosphorylation targets NPM to nuclear speckles, and (iii) Thr^{199} phosphorylation enhances the RNA-binding activity of NPM. Moreover, it has been shown that NPM is co-purified with splicing activator RNPS1 in the highly purified fractions from HeLa nuclear extracts [25]. All these findings converge to one hypothesis that NPM may be involved in pre-mRNA splicing, and such activity may be controlled by Thr^{199} phosphorylation. To test this, we first examined the physical interaction between NPM and splicing factors other than RNPS1. The HeLa nuclear extracts were immunoprecipitated with antibodies to hnRNP I and SF2/ASF. The immunoprecipitates were then immunoblotted with anti-panNPM antibody (Fig. 5C). NPM was co-immunoprecipitated with both hnRNP I (lane 1) and SF2/ASF (lane 2), indicating that NPM either directly or indirectly interact with these splicing factors.

We next examined the effect of phosphorylated NPM on pre-mRNA splicing in vitro. GST, GST-NPM/wt, GST-NPM/T199A and GST-NPM/T199D, which were subjected to in vitro kinase reaction in the presence or absence of CDK2/cyclin E, were added to HeLa nuclear extract, and subjected to an in vitro splicing assay using β-globin pre-mRNA as a substrate (Fig. 5D). Similar levels of the β-globin pre-mRNA spliced product were detected among the control (no GST proteins) (lane 2), GST (lanes 3–6), and unphosphorylated GST-NPM/wt (lanes 7–8). However, a significant repression in β-globin pre-mRNA splicing was detected when the GST-NPM/wt phosphorylated by CDK2/cyclin E was added (lane 10). Similarly, addition of the non-phosphorylatable GST-NPM/T199A mutant (with the kinase reaction in the presence or absence of CDK2/cyclin E) failed to repress pre-mRNA splicing (lanes 11–14), while addition of the phospho-mimetic GST-NPM/T199D mutant resulted in the strong repression of pre-mRNA splicing (lanes 16 and 18). Moreover, repression of pre-mRNA splicing by phosphorylated GST-NPM/wt and GST-NPM/T199D is dose dependent (lane 9 vs. lane 10, lane 15 vs. lane 16, lane 17 vs. lane 18). Thus, NPM, when phosphorylated on Thr^{199} by CDK2, acts as a suppressor of pre-mRNA splicing.

4. Discussion

CDK2/cyclin E-mediated phosphorylation of NPM on Thr^{199} has been shown to be a critical event in the initiation of centrosome duplication [12,13]. In this study, we examined whether CDK2/cyclin E (and A)-mediated phosphorylation of NPM on Thr^{199} affects biological events other than centrosome duplication by the use of the antibody that specifically recognizes phospho-Thr^{199} NPM. We found that phospho-Thr^{199} NPM accumulates at nuclear speckles in parallel with the well-established activation kinetics of CDK2/cyclin E and A, in which CDK2/cyclin E is activated at late G1, and CDK2/cyclin A during S and G2 phases of the cell cycle (reviewed in [37,53]). We further demonstrated that Thr^{199} phosphorylation targets NPM to the nuclear speckles. The nuclear speckles are the site of assembly and/or storage of splicing factors, supplying splicing factors to the sites of transcription. NPM re-localizes with authentic splicing factors such as SC35 from the nuclear speckles upon forced inhibition of transcription. NPM was co-purified with splicing activator in the highly purified fractions of splicing-competent nuclear extracts [25], and antibodies against several splicing factors, including SF2/ASF and RNPS1, co-immunoprecipitates NPM. All these findings point to the possibility that NPM associates with splicing factors to regulate splicing in vivo. We found that Thr^{199}-phosphorylation of NPM dramatically enhances its general RNA-binding activity. Moreover, in vitro splicing reaction of β-globin pre-mRNA was significantly repressed when phospho-Thr^{199} NPM as well as phospho-Thr^{199} mimetic NPM mutant was added to the reaction. Together with the previous finding, in which NPM induces changes in the secondary structure of RNA through physical interaction [15], our findings strongly indicate that NPM is involved in the pre-mRNA splicing process, which is controlled by Thr^{199} phosphorylation by CDK2/cyclin E (and A). At present, the molecular mechanism underlying the repression of pre-mRNA splicing by phospho-Thr^{199} NPM is not known, and we are currently testing three possibilities. The enhanced RNA-binding activity of phospho-Thr^{199} NPM may alter RNA structure, making the splice sites less accessible to splicing complexes. Alternatively, phospho-Thr^{199} NPM may inhibit the activities of splicing factors through physical interaction. Third possibility is that NPM may be involved in assembly of spliceosome. Spliceosome is a dynamic multiprotein/RNA complex, which involves >200 different proteins [54–56], and undergoes multiple assembly steps and conformational changes. Considering that NPM possesses a molecular chaperoning activity, NPM may promote a proper assembly of spliceosomes at the site of transcription, which is controlled by Thr^{199} phosphorylation by CDK2/cyclin E and A.

Finally, the cell cycle-dependent accumulation of phospho-Thr^{199} NPM at nuclear speckles mediated by CDK2/cyclin E (and A) and the involvement of phospho-Thr^{199} NPM in pre-mRNA splicing process raise the interesting question regarding to a possible link between pre-mRNA splicing and

cell cycle progression. Indeed, there is growing evidence linking these two events (reviewed in [57,58]). For instance, one of SR protein like factor SRp38 (also known as SRrp40, TASR-2, NSSR-1) was shown to act as a splicing repressor when dephosphorylated during M phase, and it was suggested that dephosphorylation of SRp38 plays a role in gene silencing during mitosis [59]. It has also been shown that the mRNA level of the SR protein, SRp20, is controlled in a cell cycle-dependent manner and activated by the CDK2/cyclin E-regulated transcription factor E2F [60]. Intriguingly, phospho-Thr^{199} NPM appears to be present in not all nuclear speckles (detected by anti-SC35 antibody): ~70% of them are positive for phospho-Thr^{199} NPM. This raises the possibility that there may be pre-mRNA splicing active and inactive loci near the nuclear speckles which are controlled in a cell cycle-dependent manner, and phospho-Thr^{199} NPM may be involved in temporal tuning of the pre-mRNA splicing activity in response to the cell cycle progression.

Acknowledgments: We thank K. George for technical assistance and Dr. N. Kleene for quantitative microscopic analysis. This work is supported in part by National Institute of Health (CA90522, CA95925 to K.F.) and Developmental Research Grant from the Sylvester Comprehensive Cancer Center (to A.M.)

References

[1] Spector, D.L., Ochs, R.L. and Busch, H. (1984) Silver staining, immunofluorescence, and immunoelectron microscopic localization of nucleolar phosphoproteins B23 and C23. Chromosoma 90, 139–148.
[2] Yung, B.Y., Busch, H. and Chan, P.K. (1985) Translocation of nucleolar phosphoprotein B23 (37 kDa/p*I* 5.1) induced by selective inhibitors of ribosome synthesis. Biochim. Biophys. Acta 826, 167–173.
[3] Herrera, J.E., Savkur, R. and Olson, M.O. (1995) The ribonuclease activity of nucleolar protein B23. Nucleic Acids Res. 23, 3974–3979.
[4] Savkur, R.S. and Olson, M.O. (1998) Preferential cleavage in pre-ribosomal RNA byprotein B23 endoribonuclease. Nucleic Acids Res. 26, 4508–4515.
[5] Umekawa, H., Sato, K., Takemura, M., Watanabe, Y., Usui, S., Takahashi, T., Yoshida, S., Olson, M.O. and Fruichi, Y. (2001) The carboxyl terminal sequence of nucleolar protein B23.1 is important in its DNA polymerase alpha-stimulatory activity. J. Biochem. 130, 199–205.
[6] Takemura, M., Sato, K., Nishio, M., Akiyama, T., Umekawa, H. and Yoshida, S. (1999) Nucleolar protein B23.1 binds to retinoblastoma protein and synergistically stimulates DNA polymerase alpha activity. J. Biochem. 125, 904–909.
[7] Okuwaki, M., Iwamatsu, A., Tsujimoto, M. and Nagata, K. (2001) Identification of nucleophosmin/B23, an acidic nucleolar protein, as a stimulatory factor for in vitro replication of adenovirus DNA complexed with viral basic core proteins. J. Mol. Biol. 311, 41–55.
[8] Borer, R.A., Lehner, C.F., Eppenberger, H.M. and Nigg, E.A. (1989) Major nucleolar proteins shuttle between nucleus and cytoplasm. Cell 56, 379–390.
[9] Valdez, B.C., Perlaky, L., Henning, D., Saijo, Y., Chan, P.K. and Busch, H. (1994) Identification of the nuclear and nucleolar localization signals of the protein p120. Interaction with translocation protein B23. J. Biol. Chem. 269, 23776–23783.
[10] Szebeni, A., Herrera, J.E. and Olson, M.O. (1995) Interaction of nucleolar protein B23 with peptides related to nuclear localization signals. Biochemistry 34, 8037–8042.
[11] Szebeni, A., Mehrotra, B., Baumann, A., Adam, S.A., Wingfield, P.T. and Olson, M.O. (1997) Nucleolar protein B23 stimulates nuclear import of the HIV-1 Rev protein and NLS-conjugated albumin. Biochemistry 36, 3941–3949.
[12] Okuda, M., Horn, H.F., Tarapore, P., Tokuyama, Y., Smulian, A.G., Chan, P.K., Knudsen, E.S., Hofmann, I.A., Snyder, J.D., Bove, K.E. and Fukasawa, K. (2000) Nucleophosmin/B23 is a target of CDK2/cyclin E in centrosome duplication. Cell 103, 127–140.
[13] Tokuyama, Y., Horn, H.F., Kawamura, K., Tarapore, P. and Fukasawa, K. (2001) Specific phosphorylation of nucleophosmin on Thr(199) by cyclin-dependent kinase 2-cyclin E and its role in centrosome duplication. J. Biol. Chem. 276, 21529–21537.
[14] Szebeni, A. and Olson, M.O. (1999) Nucleolar protein B23 has molecular chaperone activities. Protein Sci. 8, 905–912.
[15] Dumbar, T.S., Gentry, G.A. and Olson, M.O. (1989) Interaction of nucleolar phosphoprotein B23 with nucleic acids. Biochemistry 28, 9495–9501.
[16] Wang, D., Baumann, A., Szebeni, A. and Olson, M.O. (1994) The nucleic acid binding activity of nucleolar protein B23.1 resides in its carboxyl-terminal end. J. Biol. Chem. 269, 30994–30998.
[17] Okuwaki, M., Tsujimoto, M. and Nagata, K. (2002) The RNA binding activity of a ribosome biogenesis factor, nucleophosmin/B23, is modulated by phosphorylation with a cell cycle-dependent kinase and by association with its subtype. Mol. Biol. Cell 13, 2016–2030.
[18] Peter, M., Nakagawa, J., Doree, M., Labbe, J.C. and Nigg, E.A. (1990) Identification of major nucleolar proteins as candidate mitotic substrates of cdc2 kinase. Cell 60, 791–801.
[19] Chan, P.K., Liu, Q.R. and Durban, E. (1990) The major phosphorylation site of nucleophosmin (B23) is phosphorylated by a nuclear kinase II. Biochem. J. 270, 549–552.
[20] Jiang, P.S., Chang, J.H. and Yung, B.Y. (2000) Different kinases phosphorylate nucleophosmin/B23 at different sites during G_2 and M phases of the cell cycle. Cancer Lett. 153, 151–160.
[21] Szebeni, A., Hingorani, K., Negi, S. and Olson, M.O. (2003) Role of protein kinase CK2 phosphorylation in the molecular chaperone activity of nucleolar protein b23. J. Biol. Chem. 278, 9107–9115.
[22] Zhang, H., Shi, X., Paddon, H., Hampong, M., Dai, W. and Pelech, S. (2004) B23/Nucleophosmin serine 4 phosphorylation mediates mitotic functions of Polo-like kinase 1. J. Biol. Chem. 279, 35726–35734.
[23] Sakashita, E., Tatsumi, S., Werner, D., Endo, H. and Mayeda, A. (2004) Human RNPS1 and its associated factors: a versatile alternative pre-mRNA splicing regulator in vivo. Mol. Cell. Biol. 24, 1174–1187.
[24] Trembley, J.H., Tatsumi, S., Sakashita, E., Loyer, P., Slaughter, C.A., Suzuki, H., Endo, H., Kidd, V. and Mayeda, A. (2005) Activation of pre-mRNA splicing by human RNPS1 is regulated by CK2 phosphorylation. Mol. Cell. Biol. 25, 1446–1457.
[25] Mayeda, A., Badolato, J., Kobayashi, R., Zhang, M.Q., Gardiner, E.M. and Krainer, A.R. (1999) Purification and characterization of human RNPS1: a general activator of pre-mRNA splicing. EMBO J. 18, 4560–4570.
[26] Burge, C.B., Tuschl, T. and Sharp, P.A. (1999) Splicing of precursors to mRNAs by the spliceosomes in: The RNA World (Gesteland, R.F., Cech, T.R. and Atkins, J.F., Eds.), second ed, pp. 525–560, Cold Spring Harbor Laboratory Press, Cold Spring Harbor, NY.
[27] Jurica, M.S. and Moore, M.J. (2003) Pre-mRNA splicing: awash in a sea of proteins. Mol. Cell 12, 5–14.
[28] Misteli, T. (1999) RNA splicing: What has phosphorylation got to do with it?. Curr. Biol. 9, 198–200.
[29] Lamond, A.I. and Spector, D.L. (2003) Nuclear speckles: a model for nuclear organelles. Nat. Rev. Mol. Cell Biol. 4, 605–612.
[30] Misteli, T. (2000) Cell biology of transcription and pre-mRNA splicing: nuclear architecture meets nuclear function. J. Cell. Sci. 113, 1841–1849.
[31] Fakan, S. (1994) Perichromatin fibrils are in situ forms of nascent transcripts. Trends Cell Biol. 4, 86–90.
[32] Bregman, D.B., Du, L., van der, Z.S. and Warren, S.L. (1995) Transcription-dependent redistribution of the large subunit of RNA polymerase II to discrete nuclear domains. J. Cell Biol. 129, 287–298.
[33] Cmarko, D., Verschure, P.J., Martin, T.E., Dahmus, M.E., Krause, S., Fu, X.D., van Driel, R. and Fakan, S. (1999) Ultrastructural analysis of transcription and splicing in the cell nucleus after bromo-UTP microinjection. Mol. Biol. Cell 10, 211–223.

[34] Fu, X.D. and Maniatis, T. (1992) The 35-kDa mammalian splicing factor SC35 mediates specific interactions between U1 and U2 small nuclear ribonucleoprotein particles at the 3′ splice site. Proc. Natl. Acad. Sci. USA 89, 1725–1729.
[35] Desai, D., Wessling, H.C., Fisher, R.P. and Morgan, D.O. (1995) Effects of phosphorylation by CAK on cyclin binding by CDC2 and CDK2. Mol. Cell Biol. 15, 345–350.
[36] Mayeda, A. and Krainer, A.R. (1999) Mammalian in vitro splicing assays. Meth. Mol. Biol. 118, 315–321.
[37] Morgan, D.O. (1997) Cyclin-dependent kinases: engines, clocks, and microprocessors. Annu. Rev. Cell Dev. Biol. 13, 261–291.
[38] Fu, X.D. and Maniatis, T. (1990) Factor required for mammalian spliceosome assembly is localized to discrete regions in the nucleus. Nature 343, 437–441.
[39] Spector, D.L., Fu, X.D. and Maniatis, T. (1991) Associations between distinct pre-mRNA splicing components and the cell nucleus. EMBO J. 10, 3467–3481.
[40] Jimenez-Garcia, L.F. and Spector, D.L. (1993) In vivo evidence that transcription and splicing are coordinated by a recruiting mechanism. Cell 73, 47–59.
[41] Misteli, T., Caceres, J.F. and Spector, D.L. (1997) The dynamics of a pre-mRNA splicing factor in living cells. Nature 387, 523–527.
[42] Huang, S. and Spector, D.L. (1996) Intron-dependent recruitment of pre-mRNA splicing factors to sites of transcription. J. Cell Biol. 133, 719–732.
[43] Carmo-Fonseca, M., Pepperkok, R., Carvalho, M.T. and Lamond, A.I. (1992) Transcription-dependent colocalization of the U1, U2, U4/U6, and U5 snRNPs in coiled bodies. J. Cell Biol. 117, 1–14.
[44] Spector, D.L. (1996) Nuclear organization and gene expression. Exp. Cell Res. 229, 189–197.
[45] Fu, X.D. (1995) The superfamily of arginine/serine-rich splicing factors. RNA 1, 663–680.
[46] Graveley, B.R. (2000) Sorting out the complexity of SR protein functions. RNA 6, 1197–1211.
[47] Tacke, R., Chen, Y. and Manley, J.L. (1997) Sequence-specific RNA binding by an SR protein requires RS domain phosphorylation: creation of an SRp40-specific splicing enhancer. Proc. Natl. Acad. Sci. USA 94, 1148–1153.
[48] Cao, W., Jamison, S.F. and Garcia-Blanco, M.A. (1997) Both phosphorylation and dephosphorylation of ASF/SF2 are required for pre-mRNA splicing in vitro. RNA 3, 1456–1467.
[49] Xiao, S.H. and Manley, J.L. (1997) Phosphorylation of the ASF/SF2 RS domain affects both protein–protein and protein–RNA interactions and is necessary for splicing. Genes Dev. 11, 334–344.
[50] Xiao, S.H. and Manley, J.L. (1998) Phosphorylation–dephosphorylation differentially affects activities of splicing factor ASF/SF2. EMBO J. 17, 6359–6367.
[51] Liu, Q.R. and Chan, P.K. (1991) Formation of nucleophosmin/B23 oligomers requires both the amino- and the carboxyl-terminal domains of the protein. Eur. J. Biochem. 200, 715–721.
[52] Umekawa, H., Chang, J.H., Correia, J.J., Wang, D., Wingfield, P.T. and Olson, M.O. (1993) Nucleolar protein B23: bacterial expression, purification, oligomerization and secondary structures of two isoforms. Cell. Mol. Biol. Res. 39, 635–645.
[53] Reed, S.I. (1997) Control of the G1/S transition. Cancer Surv. 29, 7–23.
[54] Neubauer, G., King, A., Rappsilber, J., Calvio, C., Watson, M., Ajuh, P., Sleeman, J., Lamond, A. and Mann, M. (1998) Mass spectrometry and EST-database searching allows characterization of the multi-protein spliceosome complex. Nat. Genet. 20, 46–50.
[55] Rappsilber, J., Ryder, U., Lamond, A.I. and Mann, M. (2002) Large-scale proteomic analysis of the human spliceosome. Genome Res. 12, 1231–1245.
[56] Zhou, Z., Licklider, L.J., Gygi, S.P. and Reed, R. (2002) Comprehensive proteomic analysis of the human spliceosome. Nature 419, 182–185.
[57] Burns, C.G. and Gould, K.L. (1999) Connections between pre-mRNA processing and regulation of the eukaryotic cell cycle. Front. Horm. Res. 25, 59–82.
[58] Blencowe, B.J. (2003) Splicing regulation: the cell cycle connection. Curr. Biol. 13, R149–R151.
[59] Shin, C. and Manley, J.L. (2002) The SR protein SRp38 represses splicing in M phase cells. Cell 111, 407–417.
[60] Jumaa, H., Guenet, J.L. and Nielsen, P.J. (1997) Regulated expression and RNA processing of transcripts from the Srp20 splicing factor gene during the cell cycle. Mol. Cell Biol. 17, 3116–3124.